

THE DAMPING EFFECT ON UNSTABLE WHIRLINGS OF A SHAFT CARRYING AN UNSYMMETRICAL ROTOR

TOSHIO YAMAMOTO¹⁾ and HIROSHI ŌTA²⁾

Department of Mechanical Engineering

(Received September 21, 1967)

1. Introduction

There are in general three principal moments of inertia I_p , I_1 and I_2 about the three principal axes of inertia passing through the center of rotor. A principal moment of inertia I_p about the rotating axis of the rotor and the principal moments of inertia I_1 , I_2 about the axes perpendicular to the rotating axis are called the polar moment of inertia and the diametral moment of inertia respectively. A rotor with unequal diametral moments of inertia I_1 , I_2 is named the unsymmetrical rotor. It has been studied that, in the lateral vibrations of the shaft carrying such an unsymmetrical rotor there are twice as many natural frequencies as the number of degrees of freedom, since two free vibrations of natural frequencies p_i and $\bar{p}_i = 2\omega - p_i$ ($i=1, 2, \dots, k$; k =number of degrees of freedom; ω =rotating speed of the shaft) take place for each degree of freedom, and that the rotating shaft becomes dynamically unstable and the unstable whirls build up in the neighborhood of the major critical speeds ω_c where the relationship $p_i = \bar{p}_i = \omega_c$ holds^{1,2)} and in the neighborhood of the rotating speed ω_d where the condition $p_i = \bar{p}_j$ ($i \neq j$), *i.e.* $p_i + p_j = 2\omega_d$ is satisfied³⁾. In the present paper, the effect of damping forces on the unstable vibrations appearing in the shaft system with the unsymmetrical rotor are discussed both analytically and experimentally and it is cleared that the damping forces have a remarkable effect on the characteristics of these unstable vibrations, and the width of the unstable regions, being against expectation, can become wider under the influence of damping.

2. Characteristic equation of the vibratory shaft system carrying an unsymmetrical rotor

The motion of the unsymmetrical rotor without any static and dynamic unbalances is governed by the following differential equation referring to the coordinates fixed in space:

$$\left. \begin{aligned} W/g \cdot \ddot{x} + c_1 \dot{x} + \alpha x + \gamma \theta_x &= 0, \\ W/g \cdot \ddot{y} + c_1 \dot{y} + \alpha y + \gamma \theta_y &= 0, \\ I\ddot{\theta}_x + I_p \omega \dot{\theta}_y + c_2 \dot{\theta}_x + \gamma x + \delta \theta_x - \Delta I \frac{d}{dt} (\dot{\theta}_x \cos 2\omega t + \dot{\theta}_y \sin 2\omega t) &= 0, \\ I\ddot{\theta}_y - I_p \omega \dot{\theta}_x + c_2 \dot{\theta}_y + \gamma y + \delta \theta_y - \Delta I \frac{d}{dt} (\dot{\theta}_x \sin 2\omega t - \dot{\theta}_y \cos 2\omega t) &= 0, \end{aligned} \right\} \quad (1)$$

¹⁾ Professor.

²⁾ Assistant professor.

in which x, y are the deflections of the rotor in x, y -directions; θ_x, θ_y are components of the inclination θ of the rotor; W/g the mass of the rotor; I_p the polar moment of inertia of the rotor; $I_1, I_2 (I_1 > I_2)$ the diametral moments of inertia; $I = (I_1 + I_2)/2$ the mean value of the diametral moments of inertia I_1 and I_2 ; $\Delta I = (I_1 - I_2)/2$ the unsymmetry of the rotor, ω the rotating speed of the shaft; α, τ, δ the spring constants of the shaft; c_1, c_2 the viscous damping coefficients of the motions with respect to x, y and θ_x, θ_y severally. For convenience, the following dimension-less quantities are introduced:

$$\left. \begin{aligned} I_p/I &= i_p, \quad \Delta I/I = \Delta, \quad x/\sqrt{Ig/W} = x', \quad y/\sqrt{Ig/W} = y', \quad \sqrt{\alpha g/W} \cdot t = t', \\ \omega/\sqrt{\alpha g/W} &= \omega', \quad p/\sqrt{\alpha g/W} = p', \quad \tau/\alpha \cdot \sqrt{W/(Ig)} = \tau', \quad \delta W/(\alpha g I) = \delta', \\ c_1/\sqrt{W\alpha/g} &= c_1', \quad c_2/I \cdot \sqrt{W/(\alpha g)} = c_2'. \end{aligned} \right\} \quad (2)$$

Upon using Eq. (2) and omitting the primes on the dimension-less quantities, Eq. (1) can be written in the form

$$\left. \begin{aligned} \ddot{x} + c_1 \dot{x} + x + \tau \theta_x &= 0, \\ \ddot{y} + c_1 \dot{y} + y + \tau \theta_y &= 0, \\ \ddot{\theta}_x + i_p \omega \dot{\theta}_y + c_2 \dot{\theta}_x + \tau x + \delta \theta_x - \Delta \frac{d}{dt} (\dot{\theta}_x \cos 2\omega t + \dot{\theta}_y \sin 2\omega t) &= 0, \\ \ddot{\theta}_y - i_p \omega \dot{\theta}_x + c_2 \dot{\theta}_y + \tau y + \delta \theta_y - \Delta \frac{d}{dt} (\dot{\theta}_x \sin 2\omega t - \dot{\theta}_y \cos 2\omega t) &= 0. \end{aligned} \right\} \quad (3)$$

Considering the rotating coordinates $x', y', \theta'_x, \theta'_y$ with the shaft and assuming that the x, y axes coincide with the x', y' axes separately when $\Theta = \omega t - \pi/2$ becomes equal to zero, they are represented by

$$\left. \begin{aligned} x' &= x \cos \Theta + y \sin \Theta, & \theta'_x &= -x \sin \Theta + y \cos \Theta. \end{aligned} \right\} \quad (4)$$

Substitution of Eq. (4) into Eq. (3) yields the following equations referring to the rotating coordinate axes with ω :

$$\left. \begin{aligned} \ddot{x}' + c_1 \dot{x}' + (1 - \omega^2)x' - \omega(2\dot{y}' + c_1 y') + \tau \theta'_x &= 0, \\ \ddot{y}' + c_1 \dot{y}' + (1 - \omega^2)y' + \omega(2\dot{x}' + c_1 x') + \tau \theta'_y &= 0, \\ (1 - \Delta)\ddot{\theta}'_x + c_2 \dot{\theta}'_x + \{\delta + (i_p - 1 - \Delta)\omega^2\}\theta'_x - \omega(2 - i_p)\dot{\theta}'_y - c_2 \omega \theta'_y + \tau x' &= 0, \\ (1 + \Delta)\ddot{\theta}'_y + c_2 \dot{\theta}'_y + \{\delta + (i_p - 1 + \Delta)\omega^2\}\theta'_y + \omega(2 - i_p)\dot{\theta}'_x + c_2 \omega \theta'_x + \tau y' &= 0. \end{aligned} \right\} \quad (5)$$

Inserting the assumed solutions for free vibrations with the form

$$x' = Ae^{st}, \quad y' = Be^{st}, \quad \theta'_x = Ce^{st}, \quad \theta'_y = De^{st} \quad (6)$$

into Eq. (5), the following characteristic equation is derived:

$$\Phi = \begin{vmatrix} s^2 + c_1 s + (1 - \omega^2) & -2\omega s - c_1 \omega & \tau & 0 \\ 2\omega s + c_1 \omega & s^2 + c_1 s + (1 - \omega^2) & 0 & \tau \\ \tau & 0 & (1 - \Delta)s^2 + c_2 s + \{\delta + (i_p - 1 - \Delta)\omega^2\} & -(2 - i_p)\omega s - c_2 \omega \\ 0 & \tau & (2 - i_p)\omega s + c_2 \omega & (1 + \Delta)s^2 + c_2 s + \{\delta + (i_p - 1 + \Delta)\omega^2\} \end{vmatrix} = 0. \quad (7)$$

The above equation (7) obviously coincides with the characteristic equation obtained through the equations of motion for small deviations from steady forced vibrations of the rotor^{1,3}. Putting

$$\left. \begin{aligned} \mu &= c_1, \quad \lambda = c_2/c_1, \quad a_0 = s^2 + (1 - \omega^2), \quad b_0 = 2\omega s, \quad d_0 = s^2 + \{\delta + (i_p - 1)\omega^2\}, \\ e_0 &= (2 - i_p)\omega s \end{aligned} \right\} \quad (8)$$

where the quantity λ is called the damping ratio being important in the later discussion. Upon use of Eq. (8), Eq. (7) can be written in the form

$$\begin{aligned} \mathcal{O} &= (f_0 + \mu\phi_1 + \mu^2\phi_2)(\bar{f}_0 + \mu\bar{\phi}_1 + \mu^2\bar{\phi}_2) + \Delta^2(\varphi_0 + \mu\varphi_1 + \mu^2\varphi_2) \\ &= (f_0\bar{f}_0 + \Delta^2\varphi_0) + \mu(\bar{\phi}_1 f_0 + \phi_1 \bar{f}_0 + \Delta^2\varphi_1) + \mu^2(\bar{\phi}_2 f_0 + \phi_2 \bar{f}_0 + \phi_1 \bar{\phi}_1 + \Delta^2\varphi_2) \\ &\quad + \mu^3(\phi_1 \bar{\phi}_2 + \bar{\phi}_1 \phi_2) + \mu^4\phi_2 \bar{\phi}_2 \\ &= \mathcal{O}_0 + \mu\mathcal{O}_1 + \mu^2\mathcal{O}_2 + \mu^3\mathcal{O}_3 + \mu^4\mathcal{O}_4 = 0 \end{aligned} \quad (9)$$

in which

$$\left. \begin{aligned} \bar{f}_0 &= (a_0 \mp ib_0)(d_0 \mp ie_0) - \gamma^2, \\ \bar{\phi}_1 &= (d_0 \mp ie_0)(s \mp i\omega) + \lambda(a_0 \mp ib_0)(s \mp i\omega), \\ \bar{\phi}_2 &= \lambda(s \mp i\omega)^2, \\ \varphi_0 &= -\{s^4 + 2(1 + \omega^2)s^2 + (1 - \omega^2)^2\}(s^2 + \omega^2)^2, \\ \varphi_1 &= -2s(s^2 + 1 + \omega^2)(s^2 + \omega^2)^2, \\ \varphi_2 &= -(s^2 + \omega^2)^3. \quad (i = \sqrt{-1}) \end{aligned} \right\} \quad (10)$$

Denoting the natural frequencies referring to the coordinate axes fixed in space and the rotating coordinate axes with ω as p and p' severally, we have the relations $p = \omega + p'$, $\bar{p} = \omega - p'$, and hence f_0 , \bar{f}_0 and \mathcal{O}_0 in Eq. (10) are rewritten as follows:

$$\left. \begin{aligned} f_0(s) &= f_0(ip') = f_0\{i(p - \omega)\} = (1 - p^2)(\delta + i_p\omega p - p^2) - \gamma^2, \\ \bar{f}_0(s) &= f_0(-s) = f_0\{i(\bar{p} - \omega)\} = (1 - \bar{p}^2)(\delta + i_p\omega\bar{p} - \bar{p}^2) - \gamma^2, \\ \mathcal{O}_0(s) &= \mathcal{O}_0(ip') = f_0\bar{f}_0 + \Delta^2\varphi_0, \quad \varphi_0 = -(1 - p^2)(1 - \bar{p}^2)p^2\bar{p}^2, \end{aligned} \right\} \quad (11)$$

because of $s = ip'$. In Eq. (11), $f_0 = 0$ and $\mathcal{O}_0 = 0$ are the frequency equations for the symmetrical rotor without damping, *i.e.* in case of $\mu = 0$, $\Delta = 0$, and for the unsymmetrical rotor without damping, *i.e.* in case of $\mu = 0$, $\Delta \neq 0$, respectively.

In the first place, the damping effects on unstable vibrations appearing in the neighborhood of the rotating speed ω_d where the relationships $p_1 = \bar{p}_2$ and $p_2 = \bar{p}_1$ hold will be treated by using the characteristic equation (7). In Figs. 1 (a), (b), the $p' - \omega$ curves and $p - \omega$ curves near ω_d are shown where those for case of $\mu = 0$ and $\Delta = 0$, *i.e.* curves of $f_0 = 0$ and $\bar{f}_0 = 0$, are indicated by chain line curves. There is the unstable region in which the two vibrations with frequencies P_1 ($\doteq p_1$) and P_2 ($\doteq p_2$) build up exponentially³, the center of which is at ω_d where

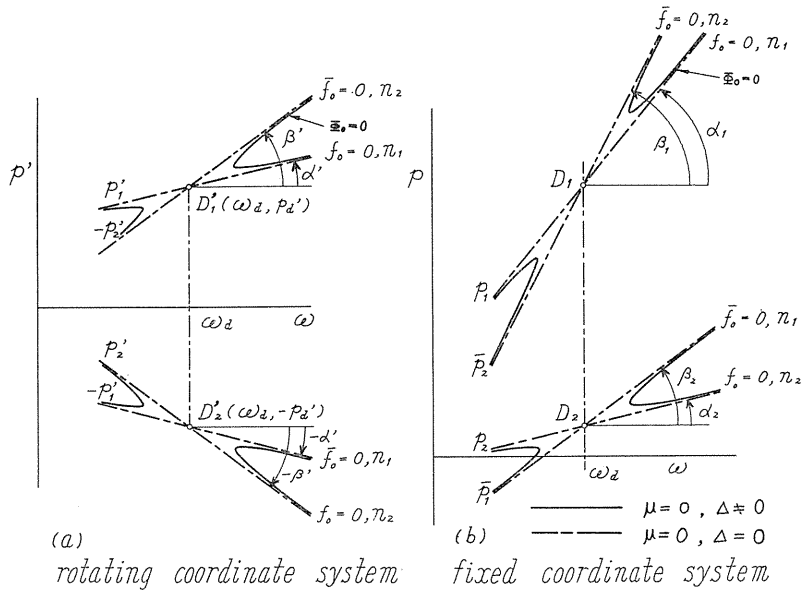


FIG. 1. $p'-\omega$ and $p-\omega$ curves in the neighborhood of $\omega_d = (p_1 + p_2)/2$.

the $p'_{1,2}-\omega$ as well as $p_{1,2}-\omega$ curves cross each other as shown in Fig. 1. The $p'-\omega$, $p-\omega$ curves for the unsymmetrical rotor without damping, *i.e.* curves of $\Phi_0=0$, are represented by full line curves in Fig. 1. Developing Eq. (7), the following 8th order equation of s is obtained:

$$K'_8 s^8 + K'_7 s^7 + K'_6 s^6 + K'_5 s^5 + K'_4 s^4 + K'_3 s^3 + K'_2 s^2 + K'_1 s + K'_0 = 0. \tag{7\cdot a}$$

For stability it is required that all K'_i ($i=0, 1, 2, \dots, 7$) must be positive since $K'_8 = 1 - \Delta^2 > 0$ ($\because 2 \geq i_p \geq 2 \Delta$) and that all Hurwitz determinants H_i ($i=3, 5, 7$) with the odd number orders must be positive. The determinant H_7 with the highest order is obviously given by

$$H_7 = \begin{vmatrix} K'_7 & K'_5 & K'_3 & K'_1 & 0 & 0 & 0 \\ K'_8 & K'_6 & K'_4 & K'_2 & K'_0 & 0 & 0 \\ 0 & K'_7 & K'_5 & K'_3 & K'_1 & 0 & 0 \\ 0 & K'_8 & K'_6 & K'_4 & K'_2 & K'_0 & 0 \\ 0 & 0 & K'_7 & K'_5 & K'_3 & K'_1 & 0 \\ 0 & 0 & K'_8 & K'_6 & K'_4 & K'_2 & K'_0 \\ 0 & 0 & 0 & K'_7 & K'_5 & K'_3 & K'_1 \end{vmatrix} \tag{7\cdot b}$$

and H_3 , H_5 are the principal minors with order 3 and 5 separately. Upon use of Eq. (7), the boundaries of the unstable regions near ω_d obtained exactly by means of digital computer are illustrated for various values of the damping coefficients c_1 , c_2 in Fig. 2 where for comparison the boundaries when no damping are shown by the full line curves *A*, and Fig. 2 (a) and (b) correspond to cases where $i_p=1$ and $i_p=1.75$ severally. In Fig. 2, the full, broken and chain line curves are adopted for cases of the damping ratio $\lambda=c_2/c_1=1$ (*i.e.* $c_1=c_2$), $\lambda=\infty$ (*i.e.* $c_1=0, c_2 \neq 0$) and $\lambda=0$ (*i.e.* $c_1 \neq 0, c_2=0$) respectively. For all curves in Fig. 2 (a) and for full

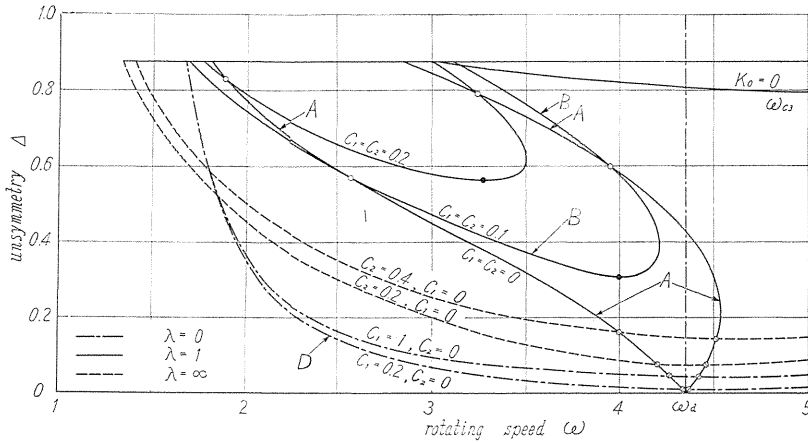
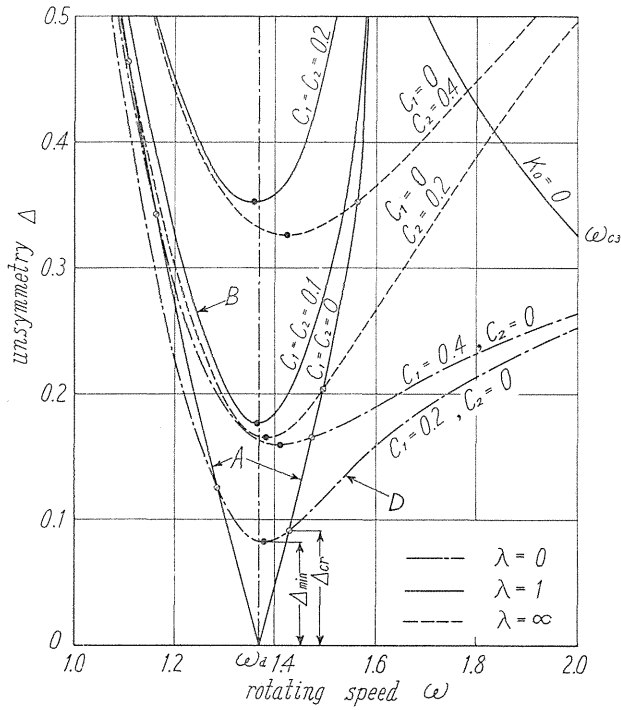


FIG. 2. Unstable regions near ω_d when there is damping or not.

line curves in Fig. 2 (b) the upper ranges closed by these curves furnish the unstable regions, and for cases of the broken and the chain line curves in Fig. 2 (b) the higher rotating speed side, *i.e.* the right hand side, means the unstable region. It is seen from Fig. 2 that the values of c_1, c_2 and λ considerably influence

on the location and the width of the unstable regions and that when the unsymmetry Δ becomes somewhat larger the unstable regions for all cases can become wider than those in case of no damping, except for cases of $\lambda=1$ ($c_1=c_2$) in Fig. 2 (a), and further that the unstable regions spread over the all higher rotating speed ranges for case of $\lambda=\infty$ or 0 ($c_1=0$ or $c_2=0$) in Fig. 2 (b).

The points at which the boundaries of the unstable regions when $\lambda=0$, $\lambda=1$ and $\lambda=\infty$ cross the curves A when no damping are shown by symbols \odot , \circ and \ominus separately in Fig. 2. Denoting the magnitude of Δ corresponding to these points as Δ_{cr} , if the unsymmetry Δ of the rotor becomes larger than this critical value Δ_{cr} the width of the unstable region when there are damping forces becomes larger than that when no damping. For example, in Fig. 2 (a) the curve D with $c_1=0.2$ and $c_2=0$ shows that the upper limit of the unstable region becomes larger than that of the curve A , provided that $\Delta > \Delta_{cr}=0.091$.

For the unstable region appearing in the neighborhood of the major critical speeds ω_c , however, the width of the unstable region are always more narrow¹⁾²⁾ than that when no damping, the reason of which will be explained later.

The symbols \bullet in Fig. 2 indicate the quantity Δ_{min} . If $\Delta < \Delta_{min}$, the unstable vibrations, and hence the unstable region cannot take place even if $\Delta \neq 0$. For instance, in case of the curve B with $c_1=c_2=0.1$ in Fig. 2 (a), (b), enough magnitude of Δ to induce the unstable vibration is larger than $\Delta_{min}=0.176$ when $i_p=1$ and $\Delta_{min}=0.308$ when $i_p=1.75$.

Incidentally, the curves $K_0=0$ in Fig. 2 illustrates the lower limit of the unstable region appearing in the neighborhood of the higher major critical speed ω_c where ω becomes equal to p_1 .

It should be noted that in the present section that quantities c_1 , c_2 , μ and Δ are considered as those with zero order and not small quantities.

3. Damping coefficients of the system with the symmetrical rotor

The damping coefficients in free vibrations of the symmetrical rotor will be simply discussed in this section, since they are necessary for the later discussion of the unstable vibrations of the unsymmetrical rotor.

The characteristic equation for the damped system of the symmetrical rotor

$$f_0 + \mu\psi_1 + \mu^2\psi_2 = 0 \quad (9 \cdot a)$$

is obtained from Eq. (9). Assuming that μ is a small quantity, and hence that the root s of Eq. (9·a) can be represented by $s=ip'+\eta$ where η is the small deviation from the characteristic root ip' in case of $c_1=c_2=0$, referring the relationships of Eq. (10) and further rejecting all higher order terms of small quantities, we obtain

$$\left. \begin{aligned} \eta &= -\mu\psi_1 / \left(\frac{\partial f_0}{\partial s} \right) = -\mu \frac{p\{(d_0 + ie_0) + \lambda(a_0 + ib_0)\}}{2p\{(d_0 + ie_0) + (a_0 + ib_0)\} - i_p \omega(a_0 + ib_0)} \\ &= -n = -(n' + n''), \\ n' &= \frac{\gamma^2 c_1}{2\gamma^2 + (1-p^2)^2(2 - i_p \omega/p)}, \quad n'' = \frac{c_2}{2\gamma^2 + (1-p^2)^2 + (2 - i_p \omega/p)}. \end{aligned} \right\} \quad (12)$$

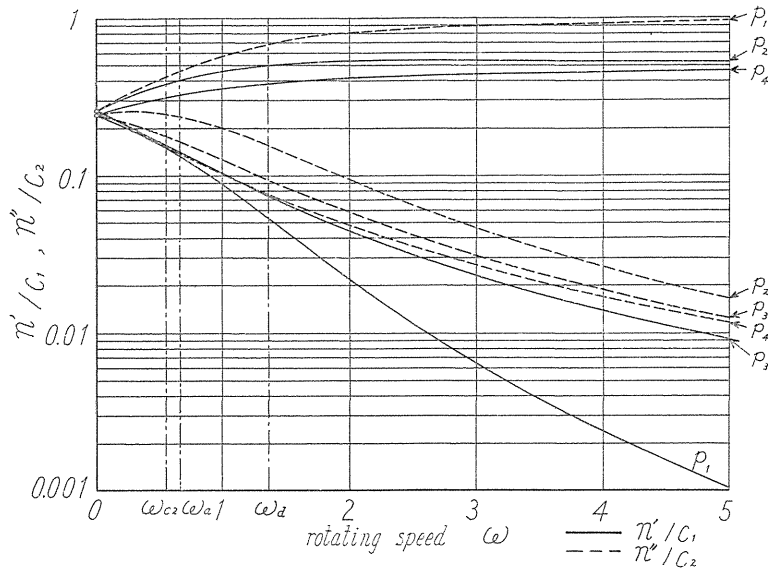


FIG. 3. Effects of ω and p_i ($i=1\sim 4$) on the magnitudes of damping coefficients n', n'' . ($i_p=1, \delta=1.060, \gamma^2=0.731, \Delta=0$)

It can be verified through general discussions of the nature for the vibratory shaft system with a symmetrical rotor that $\eta, -n, -n'$ and $-n''$ take always the negative values for any value of the rotating speed ω , and this fact is a natural consequence, since the vibratory shaft system carrying a symmetrical rotor has no unstable region and then becomes a damped system if external damping forces exist. In Eq. (12), n' and n'' mean the damping coefficients induced by c_1 and c_2 respectively. Inserting, for example, any rotating speed ω and $p=p_i$ in Eq. (12), the damping coefficient for the free vibration with the frequency p_i is derived. The influences of the kinds of the natural frequencies $p_{1,2,3,4}$ and the magnitude of ω on the values of n', n'' are shown in Fig. 3, for case of $i_p=1, \delta=1.060, \gamma^2=0.731$ and $\Delta=0$. Fig. 3 shows that there is somewhat large difference in the damping coefficients n', n'' .

Denoting the damping coefficient n for the free vibration of p_i or p'_i as n_i , we have from Eq. (10)

$$\left. \begin{aligned} n_1 &= \mu \left(\frac{\psi_1}{\partial f_0 / \partial s} \right)_{D'_1} = \mu \left(\frac{\bar{\psi}_1}{\partial \bar{f}_0 / \partial s} \right)_{D'_2} \\ n_2 &= \mu \left(\frac{\psi_1}{\partial f_0 / \partial s} \right)_{D'_2} = \mu \left(\frac{\bar{\psi}_1}{\partial \bar{f}_0 / \partial s} \right)_{D'_1} \end{aligned} \right\} \quad (12 \cdot a)$$

and it is also observed that the damping coefficient for p_i coincides with that for \bar{p}_i (cf. Fig. 1 (a)).

4. Approximate calculation of the unstable vibrations (when both the damping coefficient μ and the unsymmetry Δ are small)

As already stated, when $\mu = \Delta = 0$ there are the intersecting points $C_{1,2}$ ($\omega = \omega_{c_{1,2}}$), $A_{1,3}$ ($\omega = \omega_a$), $D_{1,2}$ ($\omega = \omega_d$) and P_{i0} ($\omega = 0$) where the p - ω curves of $f_0 = 0$ cross those of $\bar{f}_0 = 0$. Although the approximate calculations stated in the present section can be applied to any intersecting points above mentioned, the discussion to follows is carried out mainly with respect to the intersecting points $D_{1,2}$ where $\omega = \omega_d = (p_1 + p_2)/2$. Since $f_0 = 0$ and $\bar{f}_0 = 0$ hold simultaneously at the point D'_1 ($\omega = \omega_d, s = ip'_d$) in Fig. 1, it is seen from Eq. (9) that the magnitude of Φ is as small as μ^2 provided that Δ has the same order as the small quantity μ . Accordingly, the roots ω and s of the characteristic equation $\Phi = 0$ can be written as follows:

$$\omega = \omega_d + \xi, \quad s = ip'_d + \eta \quad (13)$$

which are slightly different from ω_d and ip'_d at the point D'_1 . Developing $\Phi = 0$ at the point D'_1 , we get

$$\begin{aligned} \Phi(\omega_d + \xi, ip'_d + \eta) &= \frac{\partial f_0}{\partial s} \frac{\partial \bar{f}_0}{\partial s} \eta^2 + \left\{ \left(\frac{\partial f_0}{\partial s} \frac{\partial \bar{f}_0}{\partial \omega} + \frac{\partial \bar{f}_0}{\partial s} \frac{\partial f_0}{\partial \omega} \right) \xi \right. \\ &+ \mu \left(\frac{\partial f_0}{\partial s} \bar{\psi}_1 + \frac{\partial \bar{f}_0}{\partial s} \psi_1 \right) \eta + \frac{\partial f_0}{\partial \omega} \frac{\partial \bar{f}_0}{\partial \omega} \xi^2 + \mu \left(\frac{\partial f_0}{\partial \omega} \bar{\psi}_1 + \frac{\partial \bar{f}_0}{\partial \omega} \psi_1 \right) \xi \\ &+ \mu^2 \bar{\psi}_1 \psi_1 + \Delta^2 \varphi_0 + \dots = 0. \end{aligned} \quad (14)$$

The inclination angles α' , β' (cf. Fig. 1 (a)) of the curves $f_0 = 0$, $\bar{f}_0 = 0$ at the point D'_1 are obviously given by

$$\tan \alpha' = i \left(\frac{\partial f_0}{\partial \omega} / \frac{\partial f_0}{\partial s} \right)_{D'_1}, \quad \tan \beta' = i \left(\frac{\partial \bar{f}_0}{\partial \omega} / \frac{\partial \bar{f}_0}{\partial s} \right)_{D'_1}. \quad (15)$$

Solving for η the quadratic furnished by neglecting the higher order terms smaller than the third order in Eq. (14), we have

$$\eta = 1/2 \cdot \{ -(n_1 + n_2) + i(a + \bar{a}) \} \pm 1/2 \cdot \sqrt{\{(n_1 - n_2) - i(a - \bar{a})\}^2 + 4\mathcal{P}^2} \quad (16)$$

upon using Eqs. (12·a) and (15). In Eq. (16),

$$a = \xi \tan \alpha', \quad \bar{a} = \xi \tan \beta'$$

$$\text{and} \quad \mathcal{P}^2 = \left(\frac{-\Delta^2 \varphi_0}{\frac{\partial f_0}{\partial s} \frac{\partial \bar{f}_0}{\partial s}} \right)_{D'_1} = \left(\frac{\Delta^2 \varphi_0}{\frac{\partial f_0}{\partial p} \frac{\partial \bar{f}_0}{\partial p}} \right)_{D'_1}. \quad (16 \cdot a)$$

The quantity \mathcal{P} is always real and coincides with the maximum value of the negative damping coefficient for case of no damping³⁾, i.e. m_{\max} . Putting

$$\left. \begin{aligned} A &= 4\mathcal{P}^2 + (n_1 - n_2)^2 - (a - \bar{a})^2, \\ B &= 2(n_1 - n_2)(a - \bar{a}), \\ |A_0| &= \sqrt{(\sqrt{A^2 + B^2} + A)/2}, \\ |B_0| &= \sqrt{(\sqrt{A^2 + B^2} - A)/2}, \end{aligned} \right\} \quad (15 \cdot a)$$

we have as the real part of η

$$m - n_0 = 1/2 \cdot \{ -(n_1 + n_2) \pm |A_0| \} = 1/2 \cdot \{ -(n_1 + n_2) \pm \sqrt{(\sqrt{A^2 + B^2} + A)/2} \}, \quad (17)$$

in which the upper and lower signs of \pm correspond to m and $-n_0$ separately and $-n_0$ takes always a negative value. If m in Eq. (17) is positive the vibratory system becomes unstable. Such a m with a positive value is called "the negative damping coefficient". The quantity m takes its maximum value m_{\max} at $\omega = \omega_d$ and changes its magnitude according to ω symmetrically with respect to the line $\omega = \omega_d$, since it is a function of $\xi^2 = (\omega - \omega_d)^2$.

Upon transforming back to the original notations, the condition that the real part m of η is positive, *i.e.* the unstable condition $|A_0| > (n_1 + n_2)$ is written in the form

$$F^2 > n_1 n_2 \left\{ 1 + \frac{(\tan \alpha' - \tan \beta')^2 \xi^2}{(n_1 + n_2)^2} \right\} \quad (18)$$

If the detuning $\xi = (\omega - \omega_d)$ from the center of the unstable region ω_d is not so large that the unstable condition (18) is satisfied, the system is set in the unstable region. The unstable condition when no damping, *i.e.* $A > 0$ is rewritten as follows:

$$F^2 > 1/4 \cdot (\tan \alpha' - \tan \beta')^2 \xi^2 \quad (18 \cdot a)$$

If the relationship

$$F = \sqrt{n_1 n_2} \quad (19)$$

is satisfied, the maximum value of m , *i.e.* m at $\omega = \omega_d$ vanishes. Then it follows that the unstable region does not appear if F (*i.e.* m_{\max} when no damping) is smaller than $\sqrt{n_1 n_2}$. Obviously the inequalities (18), (18·a) change into the equations on the boundaries of the unstable region and these equations yield

$$\xi_0 = \pm \sqrt{\frac{(n_1 + n_2)^2}{n_1 n_2} \left\{ \frac{-\Delta^2 \varphi_0}{\frac{\partial f_0}{\partial s} \frac{\partial \bar{f}_0}{\partial s}} - n_1 n_2 \right\}} / |\tan \alpha' - \tan \beta'|, \quad (20)$$

$$\xi_0 = \pm 2\Delta \sqrt{\frac{-\varphi_0}{\frac{\partial f_0}{\partial s} \frac{\partial \bar{f}_0}{\partial s}}} / |\tan \alpha' - \tan \beta'| = \pm 2\Delta \sqrt{\frac{\varphi_0}{\frac{\partial f_0}{\partial p} \frac{\partial \bar{f}_0}{\partial p}}} / |\tan \alpha_1 - \tan \beta_1| \quad (20 \cdot a)$$

in which ξ_0 furnishes the upper and lower boundaries of the unstable region, and Eq. (20·a) furnishing the boundaries when no damping has already been obtained in the previous paper³⁾. For damped system there is a quantity Δ_{\min} as shown in Fig. 2 and the unstable vibrations can not take place if $\Delta < \Delta_{\min}$. This quantity Δ_{\min} is obtained by putting $\xi = 0$ in Eq. (18) as follows:

$$\Delta_{\min} = \sqrt{-\frac{\partial f_0}{\partial s} \frac{\partial \bar{f}_0}{\partial s} n_1 n_2 / \varphi_0} \quad (19 \cdot a)$$

The above relationship can also be introduced from Eq. (19).

Equating ξ_0 in Eq. (20) to that in Eq. (20•a), we have the relation between Δ_{cr} and Δ_{min} as follows:

$$\Delta_{cr} = \Delta_{min} \left| \frac{n_1 + n_2}{n_1 - n_2} \right| \tag{21}$$

As already explained in Section 2, the unstable region of the damped system can be wider than that of the no damping system if $\Delta > \Delta_{cr}$.

The frequency P' of the unstable vibrations will be obtained, which is obviously the sum of p'_d and the imaginary part of η in Eq. (16), it follows that

$$P' = p'_d + 1/2 \cdot (\tan \alpha' + \tan \beta') \xi \pm 1/2 \cdot \sqrt{(\sqrt{A^2 + B^2} - A)/2} \tag{22}$$

The above discussion in this matter can be made at the intersecting point $D'_i(\omega_d, -ip'_d)$ as well as the point $D'_i(\omega_d, ip'_d)$.

If only the natural frequency p_i is once determined through Eq. (11), n_i and α', β' are given by Eqs. (12) and (15) respectively, and upon using these values $m, \xi_0, \Delta_{min}, \Delta_{cr}$ and P' of the unstable vibrations of the unsymmetrical rotor with damping can approximately be given by Eqs. (17), (20), (19•a), (21) and (22) severally, provided that the damping coefficients and the unsymmetry are small;

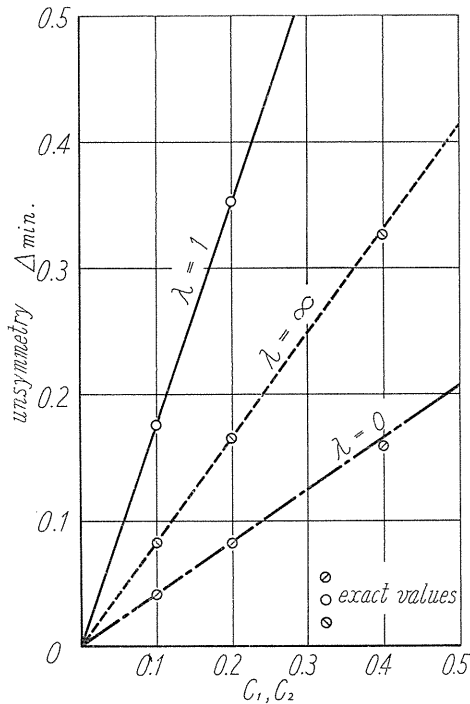


FIG. 4. Minimum value of unsymmetry Δ_{min} which yields unstable region near ω_a . ($i_p=1, \delta=1.060, \gamma^2=0.731$)

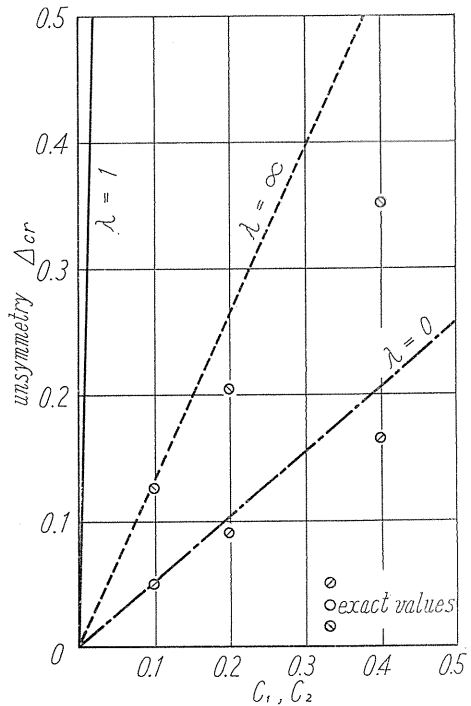


FIG. 5. Critical value of unsymmetry Δ_{cr} which makes wide or narrow the width of unstable region near ω_a due to damping. ($i_p=1, \delta=1.060, \gamma^2=0.731$)

according to whether $\Delta \geq \Delta_{\min}$ or $\Delta < \Delta_{\min}$, the unstable vibrations take place or not. It can also be observed in Fig. 4 that the approximate values of Δ_{\min} of Eq. (19.a) shown by the straight lines agree with its exact values illustrated by the circular symbols. The approximate and exact values of Δ_{cr} are shown by the straight lines and circular symbols severally in Fig. 5 in which the approximate values of Δ_{cr} given by Eq. (21) differ from the exact values when c_1, c_2 are somewhat large, since the difference of the rotating speed ω at Δ_{cr} from ω_d increases.

A new quantity Δ_{ξ} may be introduced: the unstable vibrations occur or not at the rotating speed ω where the detuning is ξ , *i.e.* at $\omega = \omega_d + \xi$ according to whether $\Delta \geq \Delta_{\xi}$ or $\Delta < \Delta_{\xi}$. Such a critical value Δ_{ξ} is obviously obtained by replacing an unequal sign by an equal sign in Eq. (18), as follows:

$$\Delta_{\xi}^2 = \Delta_{\min}^2 + g(\lambda) \left\{ -\frac{\partial f_0}{\partial s} \frac{\partial \bar{f}_0}{\partial s} / (-\varphi_0) \right\} (\tan \alpha' - \tan \beta')^2 \xi^2 \tag{18\cdot b}$$

where

$$g(\lambda) = \frac{n_1 n_2}{(n_1 + n_2)^2}.$$

It should be noted that Δ_{ξ} is not only the function of the damping coefficients c_1, c_2 but also of the damping ratio $\lambda (=c_2/c_1)$, since $g(\lambda)$ is the function of λ . Accordingly, the value Δ_{ξ} for the case $c_1 \rightarrow 0, c_2 \rightarrow 0$ in Eq. (18.b) does not coincide with that of the unstable vibrations without damping induced by Eq. (18.a), with one exception: both values of Δ_{ξ} agree each other for the case $n_1 = n_2$ with $g(\lambda) = 1/4$. In Fig. 6, Δ_{ξ} for $\xi = 0.2$ are indicated and the symbol \circ in the figure gives the value Δ_{ξ} for the no damping system which is obtained from Eq. (18.a). In Fig. 6, only the curve for $\lambda = 1$ approximately joints in the circular symbol \circ at $c_{1,2} = 0$, since in this system the relation $n_1 = n_2$ is satisfied when $\lambda = 0.84$ which is nearly equal to $\lambda = 1$. Remarkable effects of the magnitude of λ on the values of $\Delta_{\min}, \Delta_{cr}, \Delta_{\xi}$ are illustrated in Fig. 7 where $\lambda/(1+\lambda)$ is adopted as the abscissa, by means of which all ranges from $\lambda = 0$ to $\lambda = \infty$ are covered.

By putting $f_0 = \bar{f}_0, \omega = \omega_c = p$, and $p'_d = 0$, all analytical results obtained through the above discussion of the unstable vibrations in the neighborhood of the point D_1 can be applied for those in the neighborhood of

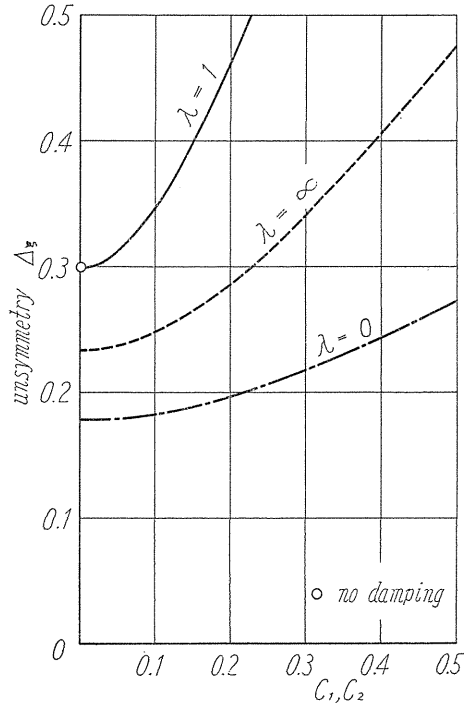


FIG. 6. Minimum value of unsymmetry Δ_{ξ} which yields unstable vibrations at the rotating speed $\omega = \omega_d + \xi$. ($i_p = 1, \delta = 1.060, \gamma^2 = 0.731, \omega_d = 1.3674, \xi = 0.2$)

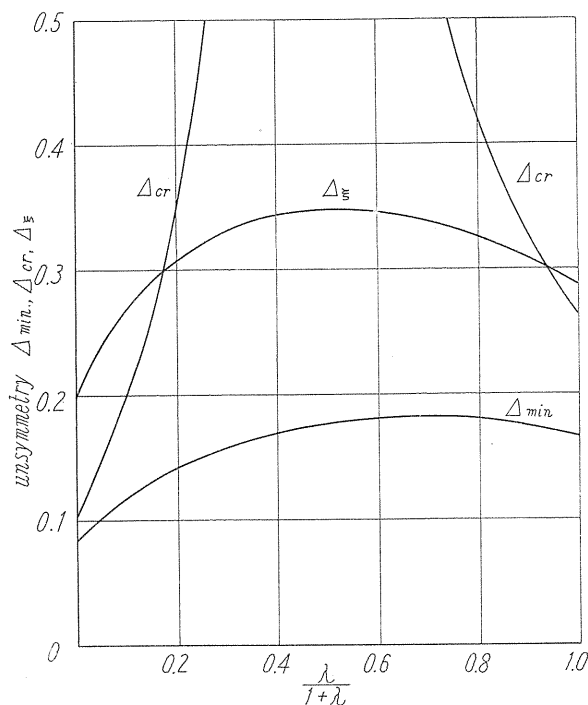
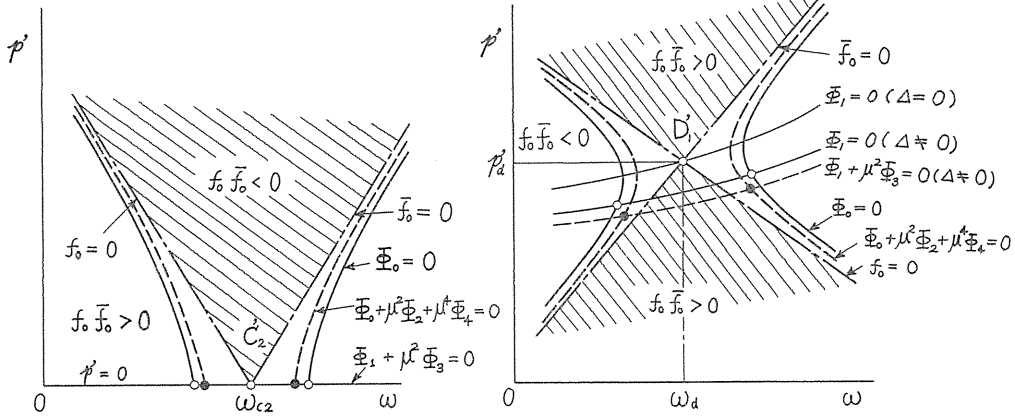


FIG. 7. The relations between Δ_{min} , Δ_{cr} , Δ_{ξ} and $\lambda/(1+\lambda)$.
 ($i_p=1$, $\delta=1.060$, $\gamma^2=0.731$, $\lambda=c_2/c_1$, $c_1+c_2=0.2$, $\xi=0.2$)

the major critical speed ω_c . For example, since the results of $p_2=\omega_c=0.736$, $\xi_0=\pm 0.148\Delta$ and $m_{max}=0.1056\Delta$ are obtained with respect to the neighborhood of the point C_2 for the no damping system with $i_p=1.987$, $\delta=1.060$, $\gamma^2=0.731$, and hence $n_2=0.50012c_1+0.14272c_2$ is derived from Eq. (12), and further as the critical viscous damping coefficients $c_{c_1}=0.164\Delta$ (when $\lambda=1$), $c_{c_1}=0.211\Delta$ (when $\lambda=0$), $c_{c_2}=0.740\Delta$ (when $\lambda=\infty$) are given by Eq. (19). These values agree with the results in Fig. 3 of the previous paper²⁾ provided Δ is not so large.

5. Graphical discussion of the unstable regions (when the damping coefficient μ is small, while the unsymmetry Δ is not small)

Although the systems in which both μ and Δ can be considered as small are treated in the preceding section, the unstable regions of the system with the large Δ under the influences of the small damping forces will be discussed in this section by means of graphical treatments. It is seen from Eq. (8) that, if the characteristic root is a pure imaginary, *i.e.* $s=ip'$, all $f_0, \bar{f}_0, \psi_2, \bar{\psi}_2, \varphi_0, \varphi_2, \Phi_0, \Phi_2, \Phi_4$ and all $\phi_1, \bar{\varphi}_1, \varphi_1, \Phi_1, \Phi_3$ in Eqs. (9), (10) become real and imaginary severally. The rotating speed ω making the root of $\Phi=0$ in Eq. (9) to be pure imaginary is obviously the boundary between the stable and unstable regions. The location of this pure imaginary (ω, ip') or (ω, p) in the p' - ω or p - ω plane is determined by obtaining the intersecting points of the curve of the real part



(a) Unstable regions near ω_{c2} ($\varphi_0 < 0, \Phi_0 < 0, \Phi_2 > 0$ in the vicinity of the point C'_2 where the relation $p_2 = \bar{p}_2 = \omega_{c2}$ is satisfied).

(b) Unstable regions near ω_a ($\varphi_0 > 0, \Phi_0 > 0, \Phi_2 < 0$ in the vicinity of the point D'_1 where the relation $p_1 + p_2 = 2\omega_a$ is satisfied).

FIG. 8. Graphical discussions of unstable regions in the neighborhood of ω_c and ω_a .

of Φ , i.e. $\Phi_0 + \mu^2 \Phi_2 + \mu^4 \Phi_4 = 0$ and the curve of the imaginary part $\Phi_1 + \mu^2 \Phi_3 = 0$, which is shown by the symbol \bullet in Fig. 8. From Eqs. (9), (10), we have

$$\Phi_{0,2,4}(-s) = \Phi_{0,2,4}(s), \quad \Phi_{1,3}(-s) = -\Phi_{1,3}(s), \quad \Phi_{1,3}(0) = 0. \tag{9\cdot b}$$

It follows that the root of $\Phi_0 + \mu^2 \Phi_2 + \mu^4 \Phi_4 = 0$ or $\Phi_1 + \mu^2 \Phi_3 = 0$ must take the form $s = \pm i p'$, and hence p and \bar{p} becomes a pair of roots since $+p'$ and $-p'$ furnish p and \bar{p} respectively. Furthermore it is also seen that one of the roots of $\Phi_1 + \mu^2 \Phi_3 = 0$ is a vanishing root, i.e. $p' = 0$ ($p = \omega$). Since the distances between the curves of $\Phi_0 = 0$ and $\Phi_0 + \mu^2 \Phi_2 + \mu^4 \Phi_4 = 0$ and the curves of $\Phi_1 = 0$ and $\Phi_1 + \mu^2 \Phi_3 = 0$ are as small as μ^2 as is seen in Fig. 8, the intersecting point of the curves $\Phi_0 = 0$ and $\Phi_1 = 0$ can nearly furnish the boundary of the unstable region. From Eqs. (9), (10), Φ is written in the form

$$\begin{aligned} -i\Phi_1 = & p\{\lambda(1-p^2) + (\delta + i_p\omega p - p^2)\}\bar{f}_0 - \bar{p}\{\lambda(1-\bar{p}^2) + (\delta + i_p\omega\bar{p} - \bar{p}^2)\}f_0 \\ & - \Delta^2 p^2 \bar{p}^2 (p - \bar{p})(1 + p\bar{p}). \end{aligned} \tag{9\cdot c}$$

In the first place, the unstable region in the neighborhood of the major critical speed ω_c is treated. The $p'-\omega$ curves in the neighborhood of $p_2 = \bar{p}_2 = \omega_{c2}$ are shown in Fig. 8 (a) where the curves $f_0 = 0, \bar{f}_0 = 0$ are given by chain line curves and the curves $\Phi_0 = 0$ and $\Phi_0 + \mu^2 \Phi_2 + \mu^4 \Phi_4 = 0$ are represented by full and broken line curves respectively. Near the intersecting point C'_2 , φ_0 takes the negative value, and hence the real root of $\Phi_0 = 0$ does not exist in the range of $f_0 \bar{f}_0 < 0$. Since Φ_2 on the line $p' = 0$ is written as follows:

$$\Phi_2(0) = -2\lambda\omega^2 f_0(\omega) + \omega^2[\lambda(1-\omega^2) + \{\delta + (i_p - 1)\omega^2\}]^2 - \Delta^2 \omega^6, \tag{9\cdot d}$$

it can be positive near the point C'_2 when Δ is small, it follows that the curves of $\Phi_0 + \mu^2 \Phi_2 + \mu^4 \Phi_4 = 0$ locate inside the curves of $\Phi_0 = 0$ as shown in Fig. 8 (a). Thus it is concluded that the width of the unstable region of the system with damping

near the major critical speed is always smaller than that of the undamped system. Since the first term of Φ_2 in Eq. (9·d) takes the positive value at the right hand side range of the point C'_2 , and hence it makes $\Phi_2(>0)$ larger and vice versa at the left hand side range. Consequently, the curve through the points at which Δ_{\min} exist goes to the left hand side, *i.e.* to the lower rotating speed side as μ increases²⁾. While near the point C'_1 of the higher major critical speed $\omega_{c_1} (= \bar{p}_1 = \bar{p}_1)$, the circumstance is in contrast with the above¹⁾.

In the next place the unstable region near the rotating speed $\omega_d (= (p_1 + p_2)/2)$ is discussed. The p' - ω diagram in the neighborhood of ω_d is shown in Fig. 8

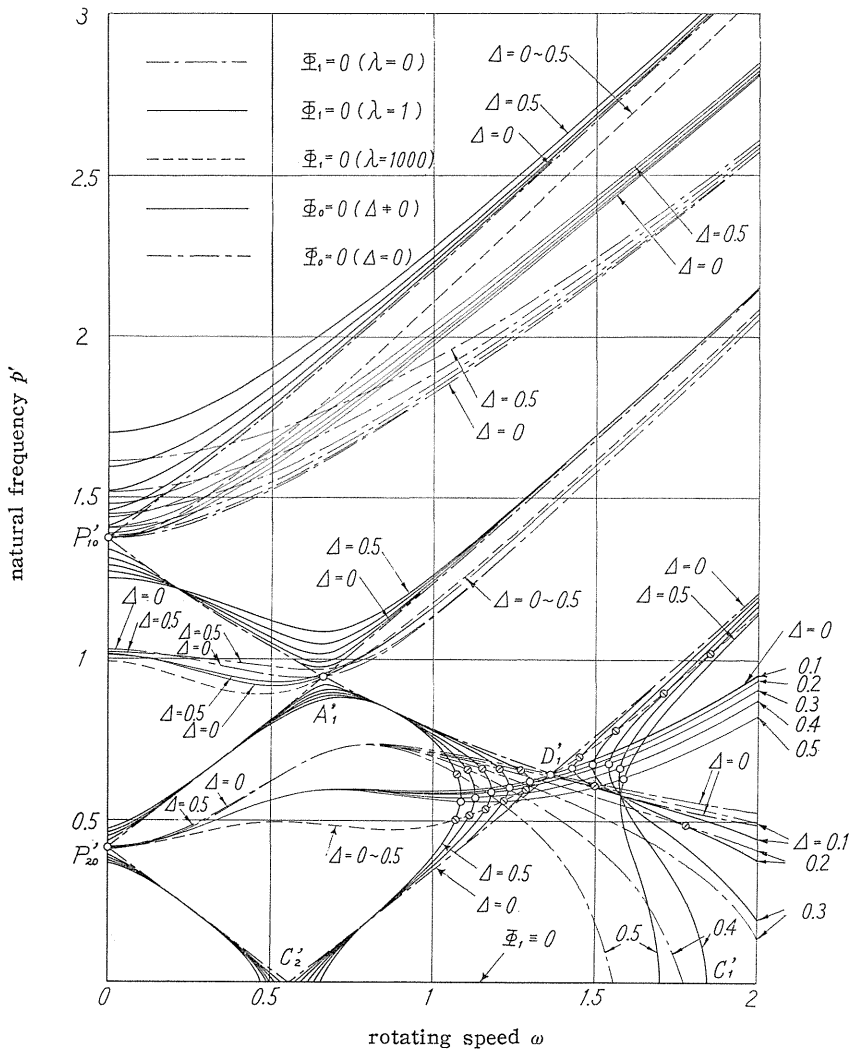


FIG. 9. (a) $i_p=1, \delta=1.060, r^2=0.731 (\omega_0=0.5571, \omega_1=0.6636, \omega_2=1.3674),$

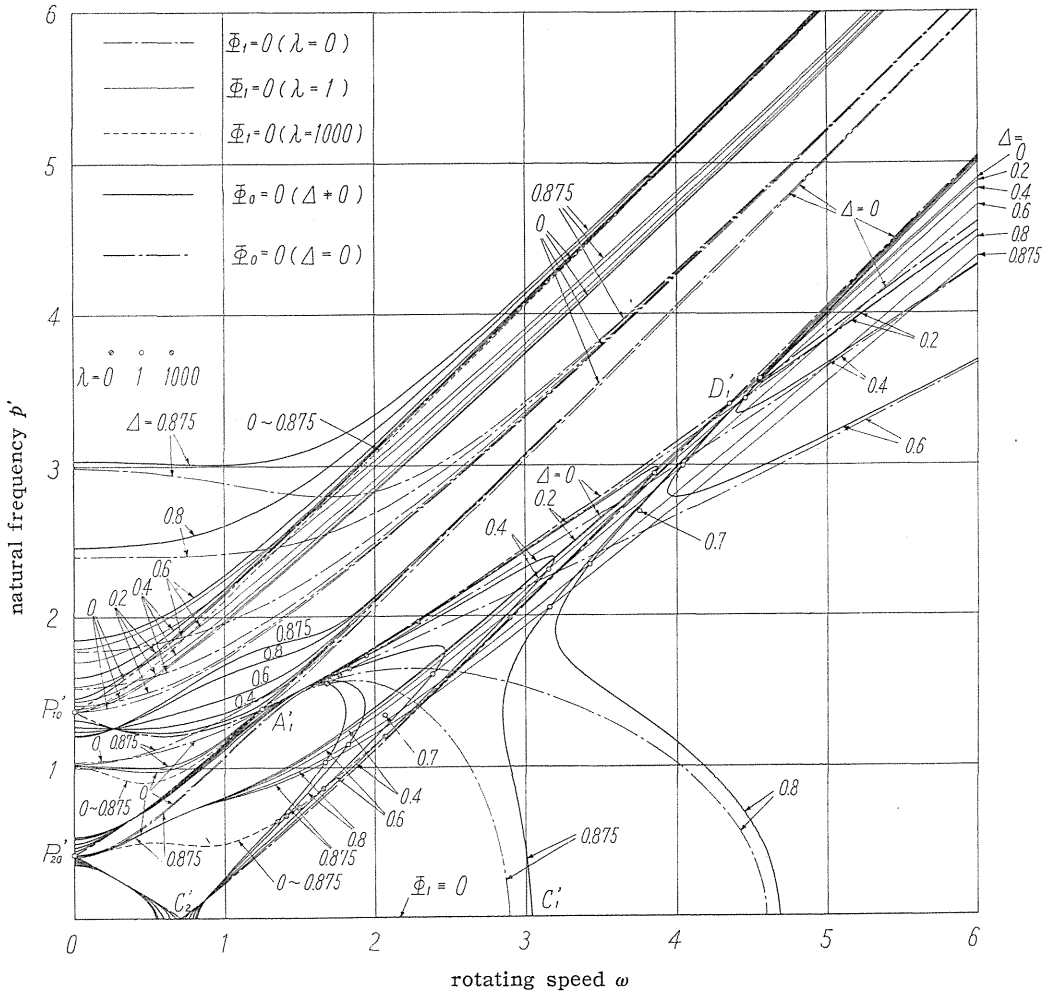


FIG. 9. (b) $i_p=1.75, \delta=1.060, \gamma^2=0.731$ ($\omega_c=0.6980, \omega_a=1.2511, \omega_d=4.3503$).

FIG. 9. Curves of $\Phi_0=0$ and $\Phi_1=0$, and their intersecting points.

(Intersecting points are indicated by marks \odot ($\lambda=0$), \circ ($\lambda=1$), \ominus ($\lambda=1000$)).

(b). The curves of $\Phi_0 + \mu^2 \Phi_2 + \mu^4 \Phi_4 = 0$ also locate inside the curves $\Phi_0 = 0$ in Fig. 8 (b). Although the curve $\Phi_1 = 0$ for the case $\Delta = 0$ passes through the point D'_1 as shown in Fig. 8 (b), it does not always pass near the throat of the pair of the curves $\Phi_0 = 0$ if $\Delta \neq 0$, and further the $\Phi_1 = 0$ cannot cross the curve $\Phi_0 = 0$ for some values of λ . For the same system as shown in Fig. 2, the real roots of $\Phi_0 = 0$ and $\Phi_1 = 0$ obtained by Eqs. (11), (9·c) are represented in Fig. 9, where the curves $\Phi_0 = 0$ are represented by thick full lines and the curves $\Phi_1 = 0$ for cases $\lambda = 0$, $\lambda = 1$ and $\lambda = 1000$ and their intersecting points are illustrated by thin chain, full and broken lines and by the symbols \odot , \circ and \ominus respectively. Some unstable regions furnished by these intersecting points considerably differ from those for no damping system which are determined by the points where the tangents on

the curve p' of the roots of $\vartheta_0=0$ become vertical. Especially when c_1 or c_2 vanishes, such a difference is remarkable. In Eq. (9.c) $\lambda=1000$ is considerably larger than Δ^2 , it follows that the broken line curves of $\vartheta_1=0$ in Fig. 9 are common for various values of Δ . In Fig. 9 (a), the curves with $\lambda=0$ do not cross the curves $\vartheta_0=0$ with $\Delta=0.3\sim 0.5$ in the higher rotating speed side of D'_1 , and in Fig. 9 (b) the curves with $\lambda=0$ and $\lambda=1000$ also have no intersecting point in the higher rotating speed side. This fact corresponds obviously to Fig. 2 in which all higher rotating speed ranges become unstable for $\lambda=0$ and ∞ . The rotating speeds of the intersecting points in the lower side are $\omega=1.68$ (when $\lambda=0$), $\omega=1.67$ (when $\lambda=1$) and $\omega=1.35$ (when $\lambda=1000$) for $\Delta=0.875$; these values coincide with the lower limits ω_{d_1} of the unstable region for $\Delta=0.875$ in Fig. 2 (b).

6. The amplitude ratio and the initial conditions in the free vibrations

The characteristic equation derived by the equations of motion which are induced by adopting the coordinates $z=x'+iy'$, $\bar{z}=x'-iy'$, $\theta_z=\theta'_x+i\theta'_y$ and $\bar{\theta}_z=\theta'_x-i\theta'_y$ in place of x' , y' , θ'_x and θ'_y in Eq. (5) has always the roots of conjugate complex s , \bar{s} , since it has real coefficients. The amplitude ratios among z , \bar{z} , θ_z and $\bar{\theta}_z$ are furnished by the ratios among the cofactors A_{1j} ($j=1, 2, 3, 4$) of this characteristic determinant. These cofactors are given as follows:

$$\left. \begin{aligned} A_{11} &= M_1 + iM_2 = \{a_0 - ib_0 + \mu(s - i\omega)\} \{ (d_0 + \lambda\mu s)^2 + (e_0 + \lambda\mu\omega)^2 - \Delta^2(s^2 + \omega^2)^2 \} \\ &\quad - \gamma^2 \{ d_0 + ie_0 + \lambda\mu(s + i\omega) \}, \\ A_{12} &= N_1 + iN_2 = \gamma^2 \Delta (s^2 + \omega^2), \\ A_{13} &= \gamma^3 - \gamma \{ a_0 - ib_0 + \mu(s - i\omega) \} \{ d_0 - ie_0 + \lambda\mu(s - i\omega) \}, \\ A_{14} &= -\gamma \Delta \{ a_0 - ib_0 + \mu(s - i\omega) \} (s^2 + \omega^2). \end{aligned} \right\} (23)$$

Assuming that the characteristic roots of conjugate complex in the stable region are represented by

$$s = -n + ip', \quad \bar{s} = -n - ip' \quad (24)$$

and referring the relations of Eq. (24) and Eq. (4) in which x' , y' are both real, the free vibrations for each degree of freedom can be written in the form

$$\left. \begin{aligned} x &= e^{-nt} \left\{ E \frac{\cos}{\sin} (pt + \alpha) + \bar{E} \frac{\cos}{\sin} (\bar{p}t - \alpha') \right\}, \\ \theta_x &= e^{-nt} \left\{ F \frac{\cos}{\sin} (pt + \gamma) + \bar{F} \frac{\cos}{\sin} (\bar{p}t - \gamma') \right\}, \end{aligned} \right\} (25)$$

where

$$\left. \begin{aligned} \bar{E} &= 4\sqrt{(L_1N_1 - L_2N_2)^2 + (L_2N_1 + L_1N_2)^2} = \sqrt{\frac{N_1^2 + N_2^2}{M_1^2 + M_2^2}} \cdot E = \frac{|A_{12}|}{|A_{11}|} E, \\ \alpha' &= \tan^{-1} \left(\frac{L_2N_1 + L_1N_2}{L_1N_1 - L_2N_2} \right) = \alpha + \arg A_{12} - \arg A_{11}. \end{aligned} \right\} (25 \cdot a)$$

In the above equations, L_1 , L_2 are arbitrary constants determined by initial conditions, M_1 , M_2 , N_1 , N_2 are real, $|A_{12}|$ and $\arg A_{12}$ are the absolute value and the argument of the complex number A_{12} separately. When there is no damping, we have $\mu=0$, $n=0$, and hence the root s becomes a pure imaginary number, it follows that all cofactors in Eq. (23) are real and $\bar{E}/E=N_1/M_1$, $\alpha'=\alpha$. A similar statement can obviously be made for the vibrations of θ_x , θ_y .

In the unstable region near the point $D'_1(\omega_d, ip'_d)$ the characteristic root s is already furnished: s is given by Eq. (13), *i.e.* $s = ip'_d + \eta$ and the small deviation η is determined by Eq. (16), which is rewritten in the form

$$\eta = 1/2 \cdot \{ -(n_1 + n_2) + i(a + \bar{a}) \} \pm 1/2 \cdot (A_0 + iB_0). \quad (16 \cdot b)$$

The deviation η' in the neighborhood of the point $D'_2(\omega_d, -ip'_d)$ is also derived as follows by a similar procedure:

$$\eta' = 1/2 \cdot \{ -(n_1 + n_2) - i(a + \bar{a}) \} \pm 1/2 \cdot (A_0 - iB_0). \quad (16 \cdot c)$$

Since the real and imaginary parts in Eqs. (16·b), (16·c) correspond to Eq. (17) and Eq. (22) separately, the roots s and s' near D'_1 and D'_2 can be represented

$$\left. \begin{aligned} s_1 &= m + i/2 \cdot \{ 2p'_d + (a + \bar{a}) + B_0 \}, & s'_1 &= -n_0 + i/2 \cdot \{ 2p'_d + (a + \bar{a}) - B_0 \}, \\ s_2 &= m - i/2 \cdot \{ 2p'_d + (a + \bar{a}) + B_0 \}, & s'_2 &= -n_0 - i/2 \cdot \{ 2p'_d + (a + \bar{a}) - B_0 \}, \end{aligned} \right\} \quad (26)$$

which lead to the following free vibrations:

$$\begin{aligned} x &= e^{mt} \left\{ \bar{E} \frac{\cos}{\sin} (P_1 t + \alpha) + \bar{E} \frac{\cos}{\sin} (P_2 t - \alpha') \right\} + e^{-n_0 t} \left\{ E' \frac{\cos}{\sin} (P'_1 t + \beta) + \bar{E}' \frac{\cos}{\sin} (P'_2 t - \beta') \right\}, \\ \theta_x &= e^{mt} \left\{ \bar{F} \frac{\cos}{\sin} (P_1 t + \gamma) + \bar{F} \frac{\cos}{\sin} (P_2 t - \gamma') \right\} + e^{-n_0 t} \left\{ F' \frac{\cos}{\sin} (P'_1 t + \delta) + \bar{F}' \frac{\cos}{\sin} (P'_2 t - \delta') \right\}, \\ \theta_y & \end{aligned} \quad (27)$$

where

$$\left. \begin{aligned} \frac{P_1}{P'_1} &= \omega + p'_d + 1/2 \cdot \{ (\tan \alpha' + \tan \beta') \xi \pm B_0 \}, & \frac{P_2}{P'_2} &= \omega - p'_d - 1/2 \cdot \{ (\tan \alpha' + \tan \beta') \xi \pm B_0 \}, \\ P_1 = \bar{P}_2 &= 2\omega - P_2, & P'_1 = \bar{P}'_2 &= 2\omega - P'_2. \end{aligned} \right\} \quad (27 \cdot a)$$

All quantities in Eq. (27) are clearly real. The amplitude ratios $E : \bar{E} : F : \bar{F}$ can be determined by using s_1 , s_2 in place of s , \bar{s} in Eqs. (23), (25·a); the ratios $E' : \bar{E}' : F' : \bar{F}'$ can also be furnished upon using s'_1 , s'_2 . In Eq. (27) the amplitudes \bar{E} , \bar{E}' , \bar{F} and \bar{F}' are in proportion to the unsymmetry Δ , and the small μ results in $\alpha \doteq \alpha' \doteq \gamma \doteq \gamma'$, $\beta \doteq \beta' \doteq \delta \doteq \delta'$ and $\alpha = \alpha' = \gamma = \gamma'$, $\beta = \beta' = \delta = \delta'$ if μ vanishes. It is also seen that both unstable vibrations of P_1 and P_2 have the common negative damping coefficient m and the vibrations of P'_1 and P'_2 have a common damping coefficient $-n_0$. The terms in $\{ \}$ of e^{mt} are determined by two initial conditions and other two initial conditions decide those in $\{ \}$ of $e^{-n_0 t}$, thus the solution of Eq. (27) are completely settled.

7. Experimental results

The analytical results obtained in the above discussions are verified by the experiments. The dimensions of the experimental apparatus are as follows³⁾:

$$\left. \begin{aligned} I_p &= 0.4300 \text{ kg cm s}^2, \quad I_1 = 0.5090 \text{ kg cm s}^2, \\ I_2 &= 0.3816 \text{ kg cm s}^2, \quad W = 11.637 \text{ kg}, \\ \alpha &= 3.120 \times 10 \text{ kg/cm}, \quad \gamma = -6.450 \times 10^2 \text{ kg/rad}, \\ \delta &= 1.777 \times 10^4 \text{ kg cm/rad}, \quad \sqrt{\alpha g/W} = 51.26 \text{ rad/s} = 489.5 \text{ r.p.m.}, \\ \sqrt{I_j/W} &= 6.124 \text{ cm}. \end{aligned} \right\} \quad (28)$$

$$i_p = 0.96593, \quad \Delta = 0.14308, \quad \delta = 15.191, \quad r^2 = 11.400, \quad \omega_d = 3.1549. \quad (28 \cdot a)$$

Substitution these values into Eqs. (7·a), (16·a), (20·a), we have

$$\omega_{d_1} = 3.1089, \quad \omega_{d_2} = 3.2030, \quad m_{\max} = 0.21932\Delta, \quad \xi_0 = \pm 0.32952\Delta. \quad (28 \cdot b)$$

The analytical results of the amplitude ratios \bar{E}/E , \bar{F}/F obtained by Eqs. (7·a), (23), (25), (27) are shown in Fig. 10. In the unstable region the values of \bar{E}/E , \bar{F}/F hold nearly constant values, and hence they can be represented approximately by those at $\omega = \omega_d$, and reciprocal relations $(\bar{E}/E)_{p_1} \cdot (\bar{E}/E)_{p_2} = 1$, $(\bar{F}/F)_{p_1} \cdot (\bar{F}/F)_{p_2} = 1$ hold. In the stable region the magnitudes of the amplitude ratios rapidly increase¹⁾ near the boundaries of the unstable region, which are usually the same order as Δ . The ratio $(\bar{E}/E)_{p_2}$ between the amplitudes of deflections with frequencies \bar{p}_2 and p_2 takes a quite small value 0.03667, while the ratio $(\bar{F}/E)_{p_2}$ between the inclination of \bar{p}_2 and the deflection of p_2 is $0.3484 \cdot \sqrt{W/(I_1)}$, i.e. $(\bar{F}/E)_{p_2} = (\bar{F}/F)_{p_2} \cdot (F/E)_{p_2} = 0.3259^\circ/\text{mm}$, which can be experimentally observed and approximately coincides with $0.411^\circ/\text{mm}$ of the results³⁾ in Experiment I of the approximately no damping system in Table 1.

In the experimental apparatus the vertical rotating shaft is supported only at the upper shaft end and the shaft with the length 31 cm is attached at the lower side of the unsymmetrical rotor, the lower end of which is submerged in damping oil by 13 cm, and hence the damping force is induced to the system. Occurrence or no occurrence of the unstable vibrations in

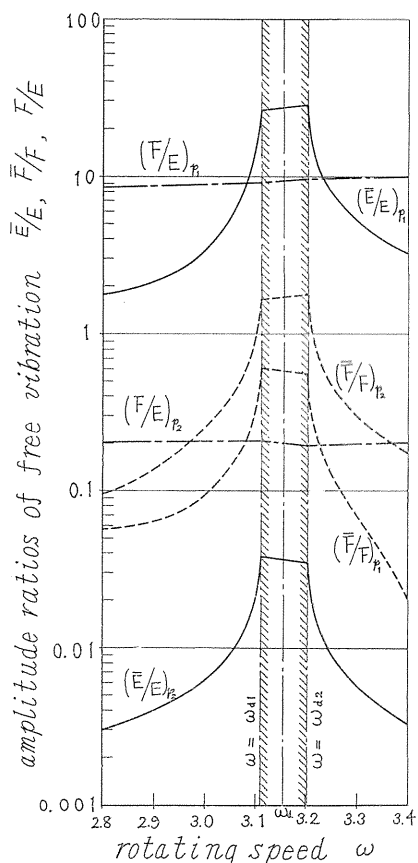


FIG. 10. Relations between amplitude ratios and rotating speed when there is no damping.

$$(i_p = 0.96593, \quad \delta = 15.191, \quad r^2 = 11.400, \\ \Delta = 0.14308, \quad c_1 = c_2 = 0, \quad \omega_{d_1} = 3.1089, \\ \omega_{d_2} = 3.1549, \quad \omega_{d_2} = 3.2030)$$

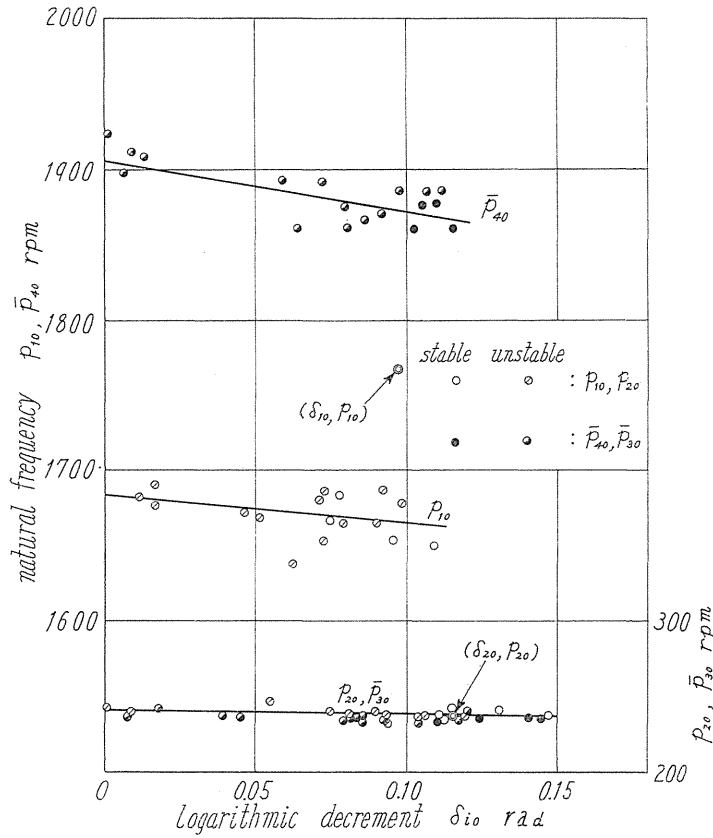


FIG. 11. Relations between natural frequency p_{i_0} and logarithmic decrement δ_{i_0} when ω is zero. (Marks \odot indicate critical values of experiment III)

the neighborhood of ω_d is assured for various viscosities of damping oil, and further the logarithmic decrement δ_{i_0} as well as the natural frequencies p_{10} , p_{20} (\bar{p}_{40} , \bar{p}_{30}) when $\omega=0$ is measured through the free vibrations in the direction of the principal moment of inertia I_1 (I_2). The relation between p_{i_0} and δ_{i_0} is shown in Fig. 11 where δ_{i_0} increases with the viscosity of oil and p_{i_0} slightly decreases. In order to determine the damping coefficients n_1 , n_2 of the symmetrical rotor we adopt the mean values of the experimentally obtained values p_{10} and \bar{p}_{40} of the unsymmetrical rotor as p_{10} which is shown in Table 1. In Table 1, the damping oil is not used in Experiment I, and its viscosity increases as in order of Experiments II, III and IV. As shown in Table 1, m_{max} decreases as the viscosity increases and the unstable vibrations can not take place in Experiment IV in which the damping oil with the highest viscosity is used. The boundary of occurrence or no occurrence of the unstable vibration seems to happen in Experiment III, p_{i_0} , δ_{i_0} of which are indicated by the symbol \odot in Fig. 11.

The relationships between the damping coefficients n_1 , n_2 of the symmetrical rotor and c_1 , c_2 are derived from Eqs. (12), (28•a) as follows:

TABLE 1. Comparisons of Calculated Values and Experimental Values for Unstable Vibrations in the Neighborhood of ω_d

	calculation of no damping	experiment I	experiment II	experiment III	experiment IV	
$A=0, \omega=0$	p_{10} rpm	2176	(1792)	(1775)	(1768)	(1705)
	p_{20} rpm	265	(240)	(239)	(238)	(233)
	δ_{10} rad	0	(0.011)	(0.073)	(0.097)	(0.34)
	δ_{20} rad	0	(0.024)	(0.069)	(0.115)	(0.34)
	c_1	0	0.00325	0.00677	0.0128	0.0341
	c_2	0	0.0133	0.0881	0.116	0.394
	$\lambda=c_2/c_1$	/	4.1	13.1	9.1	11.5
$A=0.14308, \omega=\omega_d=3.1549$	$\sqrt{n_1 n_2}$ rad/s	0	0.22	0.93	1.39	4.32
	$\mathcal{V}-\sqrt{n_1 n_2}$ rad/s	1.61	1.39	0.68	0.22	-3.71
	occurrence or no occurrence	yes	(yes)	(yes)	(critical)	(no)
	m_{\max} rad/s	1.61* 1.61**	1.34 (1.54)	0.46 (0.73)	0.14 (0)	-5.75
	$(\bar{E}/E)_{p_2}$	0.03667	0.03307	0.01766	0.01530	0.00774
	$(\bar{F}/F)_{p_2}$	1.7055	1.5307	0.7922	0.6685	0.3620
	$(F/E)_{p_2}$	0.2043	0.2042	0.2038	0.2037	0.2032
	$(\bar{F}/E)_{p_2}$ °/mm	0.3259	0.2924 (0.411)	0.1511 (0.256)	0.1274	0.0688

* approximate solution, ** exact solution, (): experimental values.

when $\omega=0$

$$\left. \begin{aligned} n_{10} &= 0.02425 c_1 + 0.47575 c_2, \\ n_{20} &= 0.47575 c_1 + 0.02425 c_2, \end{aligned} \right\} \quad (12 \cdot b)$$

when $\omega=\omega_d$

$$\left. \begin{aligned} n_1 &= 0.00743 c_1 + 0.67012 c_2, \\ n_2 &= 0.53860 c_1 + 0.02235 c_2. \end{aligned} \right\} \quad (12 \cdot c)$$

Substituting the values of c_1, c_2 obtained by Eq. (12·b) and $n_{10} = p_{10} \delta_{10} \sqrt{W/(\alpha g)}/(2\pi) = 0.0557, n_{20} = 0.00890$ given by Experiment III, *i.e.* the critical case of occurrence or not, into Eq. (12·c), we have $\sqrt{n_1 n_2} = 0.0271$ (*i.e.* 1.39 rad/s). This value well agrees with $\mathcal{V} = 1.61$ rad/s (the maximum value of the negative damping coefficient when there is no damping) as well as the experimental results $m_{\max} = 1.54$ rad/s of Experiment I, and hence it approximately satisfy the critical condition (19). As is shown in Table 1, the unstable vibrations take place in Experiments I and II since $\mathcal{V} > \sqrt{n_1 n_2}$ and not in Experiment IV³⁾ because of $\mathcal{V} < \sqrt{n_1 n_2}$; Experiment III corresponds to the case $\mathcal{V} = \sqrt{n_1 n_2}$ as above mentioned. In Table 1, the ampli-

tude ratios and m_{\max} analytically obtained are shown and those of experimental results are furnished in (), from which the effects of damping forces are clearly observed. For Experiment II, Eq. (7·b) furnishes the exact values $\omega_{d_1}=3.0885$ and $\omega_{d_2}=3.2249$ and hence $\omega_{d_2}-\omega_{d_1}=0.1364$ which is larger than $\omega_{d_2}-\omega_{d_1}=3.2030-3.1089=0.0941$ obtained by Eq. (28·a) and this fact agrees with the experimental results that the existence of damping makes the unstable region wider.*

Speaking strictly, the equations of motion for the experimental apparatus can be governed by Eq. (1) under the following five assumptions: [1] The distributed mass of the shaft is negligible, [2] the higher powers of x, y, θ_x, θ_y than the third order are also considered as negligible small, [3] the angular acceleration $\ddot{\theta}$ are as small as the second order of x, y, θ_x, θ_y and hence it can be considered as zero, [4] only the viscous damping forces in proportion to velocity $\dot{x}, \dot{y}, \dot{\theta}_x$ and $\dot{\theta}_y$ exist in the system, [5] The viscous damping coefficients c_1 and c_2 are independent of the rotating speed ω , and hence their values when $\omega=0$ can always be used.

As is seen from the above discussions the analytical and experimental results agree with each other under these assumption.

8. Conclusions

(1) The external viscous damping forces act always as the resistance to the whirling motions of the symmetrical rotor.

(2) When both the damping forces and the unsymmetry are small, the approximate analytical results of the unstable vibrations agree with both the exact analytical results and the experimental results.

(3) The negative damping coefficient m is always made smaller by the damping forces.

(4) The width of the unstable region in the neighborhood of the major critical speed ω_c is always made narrow by the damping forces, while the unstable region near the rotating speed ω_d , contrary to expectation, can become wider by the damping actions, and for some cases all the higher rotating speed regions become unstable by the damping. The width of the unstable region near ω_d is considerably influenced by the value of the damping ratio λ .

(5) Through the graphical discussion of the intersecting points of the real part $\phi_0=0$ and the imaginary part $\phi_1=0$ in the frequency equation, the conclusion stated in (4) can be made more clear.

References

- 1) T. Yamamoto and H. Ōta, "On the Vibrations of the Shaft Carrying an Asymmetrical Rotating Body". Bulletin of the Japan Society of Mechanical Engineers, Vol. 6, No. 21, 1963, pp. 29-36.
- 2) T. Yamamoto and H. Ōta, "On the Forced Vibrations of the Shaft Carrying an Unsymmetrical Rotating Body (Response Curves of the Shaft at the Major Critical Speeds)", Bulletin of the Japan Society of Mechanical Engineers, Vol. 6, No. 23, 1963, pp. 412-420.
- 3) T. Yamamoto and H. Ōta, "On the Unstable Vibrations of a Shaft Carrying an Unsymmetrical Rotor". Journal of Applied Mechanics, Trans. of the ASME, Vol. 31, Series E, No. 3, 1964, pp. 515-522.

* In Figs. 10, 12 of Reference 3), m_{\max} becomes smaller by damping, while the unstable region becomes wider by 40~50%.